

Periodic mesoporous $\text{Li}_x(\text{Mn}_{1/3}\text{Ni}_{1/3}\text{Co}_{1/3})\text{O}_2$ spinel†

Matthew R. Hill,^{*a,b} Jamie Booth,^a Laure Bourgeois^c and Harold J. Whitfield^{a,c}

Received 22nd March 2010, Accepted 19th April 2010

First published as an Advance Article on the web 7th May 2010

DOI: 10.1039/c005146m

A monoclinic periodic mesoporous $\text{Li}_x(\text{Mn}_{1/3}\text{Ni}_{1/3}\text{Co}_{1/3})\text{O}_2$ spinel has been successfully prepared for the first time using a ‘two solvents’ pore infiltration methodology on hard silica templates. More commonly used synthetic techniques are not applicable to this complex material. This important battery cathode has a surface area of over $180 \text{ m}^2\text{g}^{-1}$ and a pore size of 5.5 nm.

Introduction

In the push towards viable renewable energy technology, improved means of energy storage are crucial for offsetting the intermittent nature of sources including wind, solar, and tidal power. At the forefront of storage technologies are improved batteries, particularly Li-ion based systems, due to their high energy and power densities.¹ With reference to the development of cathode materials within these systems, recent strategies have focussed upon increasing their surface area to shorten diffusion path lengths concomitant with improved charge-discharge rates,² and creating periodic mesoporous structures to enhance cyclability whilst maintaining high surface area. Most synthetic approaches towards periodic mesoporous cathode materials^{3–6} have entailed nano-templating from either soft materials such as surfactants, colloids, and co-polymers,^{7–10} or hard materials such as carbons and silicas.^{6,11} However, to date, none of these routes have been successfully applied to nanostructuring one of the most promising cathode materials, $\text{Li}(\text{Mn}_{1/3}\text{Ni}_{1/3}\text{Co}_{1/3})\text{O}_2$,¹² despite the success with closely related sub-component materials such as LiMnO_2 ^{13–17} and LiCoO_2 .^{18,19} The difficulties would appear to reflect several underlying materials challenges particular to complex metal oxides⁸ and phosphates. Many of these materials exhibit a strong preference for the formation of large crystallites, often related to the high temperatures of formation, hindering the growth of a contiguous structure. Furthermore, the low levels of pore filling commonly related to the templating of metal oxides compounds the challenge.

Common evaporation based pore infiltration routes have been shown to deliver filling levels as low as 24% in some cases,²⁰ whereas the ‘two solvents’ route employed in the present article, where a hydrophilic mesoporous silica template is suspended in a hydrophobic medium and an aqueous precursor solution drawn into its pores, may deliver pore filling levels as high as 97%.²¹ The higher pore filling levels are required to ensure the structure does not collapse upon template removal. Secondly, the large number of elemental components in these complex materials requires intimate mixing to occur within the confined space environment

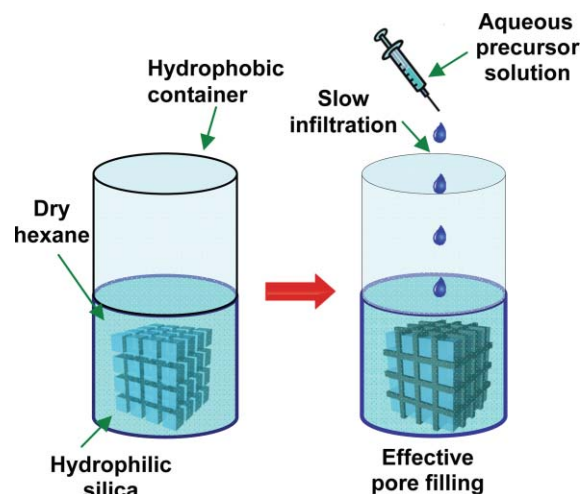


Fig. 1 The two solvents pore filling methodology.

of a template, a troublesome process if precursors exhibit varying diffusion characteristics. Finally, in the case of lithiated materials, Li-intercalation with graphitic carbon templates, or Li-extraction during dissolution of a silica template demands post-template lithiation.¹⁸

Consequently most synthetic efforts to date have produced macroporous $\text{Li}(\text{Mn}_{1/3}\text{Ni}_{1/3}\text{Co}_{1/3})\text{O}_2$ ^{22,23} which, when incorporated into composite battery electrodes, does not perform well at high rates of charging/discharging.^{12,24,25} To achieve rapid reversible electrochemical reactions at the electrode/electrolyte interface it is essential to prepare the electrode in a stable mesoporous form. Such structural configuration is especially important when the electrode materials are coupled with electrolytes where the ionic diffusion is slow.

Herein we report the novel preparation of a monoclinic $\text{Li}_x(\text{Mn}_{1/3}\text{Ni}_{1/3}\text{Co}_{1/3})\text{O}_2$ spinel phase that exhibits periodic mesoporosity. The route employed involves an adaptation and extension of the ‘two solvents’ synthetic methodology,^{21,26} and under optimised conditions leads to materials that display surface areas of more than $180 \text{ m}^2\text{g}^{-1}$. Surface areas for this material were previously limited to $24 \text{ m}^2\text{g}^{-1}$.²²

More commonly employed synthetic routes, such as pore filling of mesoporous carbon or silica templates by means of solvent evaporation from a precursor solution, led only to disordered materials for this system. The ‘two solvents’ approach, was found to be the most efficient pore filling mechanism for this system.

^aCSIRO Materials Science and Engineering, Private Bag 33, Clayton South MDC, Victoria, 3169, Australia. E-mail: matthew.hill@csiro.au

^bSchool of Chemistry, University of Melbourne, Victoria, 3010, Australia

^cMonash Centre for Electron Microscopy and Department of Materials Engineering, Monash University, Victoria, 3160, Australia

† Electronic supplementary information (ESI) available: Experimental details and supporting figures and tables. See DOI: 10.1039/c005146m

Nevertheless, two cycles of a concentrated precursor solution were required to gain sufficient pore filling to deliver structural integrity.²⁷

Lithiation was undertaken after removal of the silica template to avoid side-reactions. Fig. 2 shows that the preparative route employed leads to a nanocrystalline material with a phase that is most likely a spinel of $\text{Li}_x(\text{Mn}_{1/3}\text{Ni}_{1/3}\text{Co}_{1/3})\text{O}_2$. Scherrer analyses confirmed the nanocrystalline nature of the material, with crystallites typically in the range of 7–9 nm in periodically mesoporous samples derived from calcination at 500–700 °C. Higher calcination temperatures (over 800 °C) resulted in significant crystallization to deliver crystallites over 80 nm in size, causing collapse of the mesoporous structure. Elemental analyses (ICP) indicated that the materials obtained were of a stoichiometric composition $\text{Li}_x(\text{Mn}_{1/3}\text{Ni}_{1/3}\text{Co}_{1/3})\text{O}_2$, where x ranges from 0.33 to 0.40 (see supplementary information†). The lower lithiation level may be in line with other phases formed at low temperatures in this family of materials.^{13,17,29} As a result of the low calcination temperatures and diminished lithium content, it is most likely that the phase obtained is a spinel, based on the results of related preparations.¹⁷ However, the broadness of diffraction peaks due to the small crystallite size precludes an indexing of the unit cell, or detailed comparison to layered structures as the diffraction patterns are likely to be very similar.^{12,17}

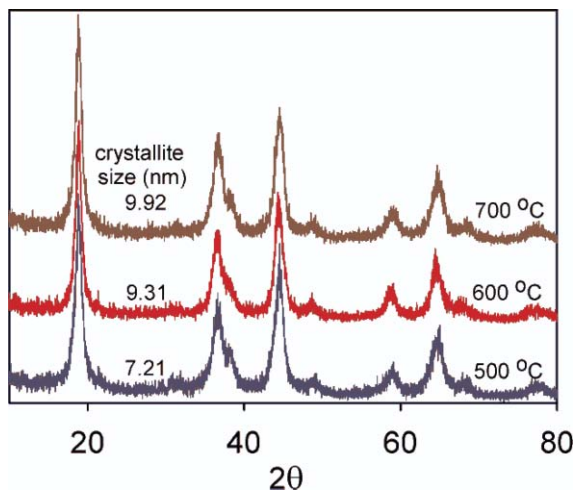


Fig. 2 XRD patterns of periodic mesoporous $\text{Li}_x(\text{Mn}_{1/3}\text{Ni}_{1/3}\text{Co}_{1/3})\text{O}_2$ as a function of calcination temperature (top). Inset: crystallite size as determined through Rietveld analyses.²⁸

TEM was employed to monitor the degree of pore infiltration by the mixed metal nitrate precursor solution, with dark regions representing the complex metal oxide (Fig. 3). Micrographs following one infiltration cycle indicated the presence of extensive voids in the structure (Fig. 3, top left), whereas a contiguous structure was observed following a second infiltration cycle (Fig. 3, top right) that delivered a material with ordered mesoporosity after template removal (Fig. 3, bottom).

Fig. 4 (top, triangles) illustrates the high surface area of the materials developed. As the amount of infiltrant was increased, there was a corresponding increase in surface area until the second pore filling cycle ($2 \times 5 \text{ mol L}^{-1}$) where a slight decrease occurred due to the formation of a contiguous structure as opposed to discrete nanoparticles. Calcination caused a linear decrease in

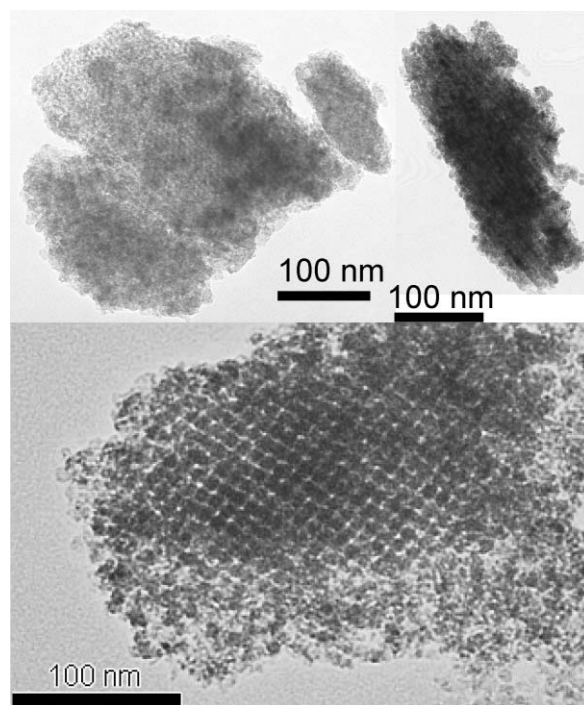


Fig. 3 TEM images of periodic mesoporous $\text{Li}_x(\text{Mn}_{1/3}\text{Ni}_{1/3}\text{Co}_{1/3})\text{O}_2$.

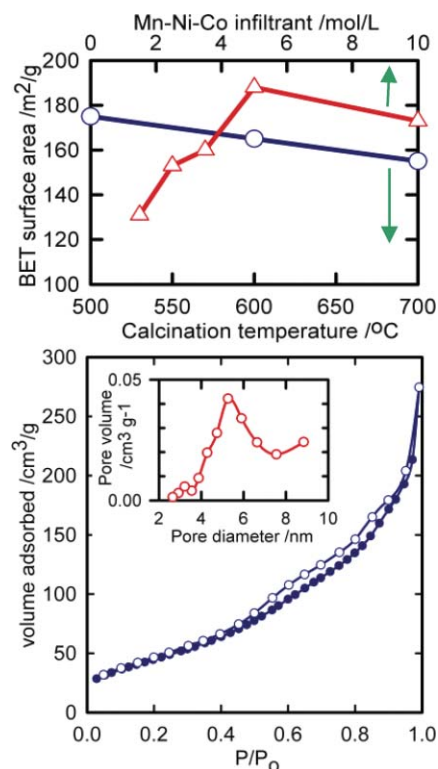


Fig. 4 Top: effect of infiltrant quantity on BET surface area (triangles) and calcination temperature (circles). Bottom: a typical N_2 sorption isotherm exhibiting (inset) a pore size distribution centred at 5.5 nm from the BdB-FHH method.^{30,31}

surface area due to crystallization (Fig. 4, top, circles). Treatment at 800 °C resulted in reaction with the template, as evidenced by formation of a low density grey material, presumably a silicate.³⁰

Higher temperatures led to complete collapse of the nanostructure and a material with $\sim 1 \text{ m}^2\text{g}^{-1}$ surface area. A typical N_2 sorption isotherm is shown in Fig. 4 (bottom). The material exhibits a high surface area with a mesopore size centred at 5.5 nm (BdB-FHH method, Fig. 4, inset).

In order to most effectively characterize the phase of the material produced at these low calcination temperatures, selected area electron diffraction (SAED) was combined with a refinement of synchrotron XRD patterns (Fig. 1). SAED of a collection of crystallites delivered diffraction rings as shown in Fig. 5. Convergent beam diffraction of individual crystals led to structural changes due to the intensity of the beam. The SAED data, when examined in concert with the XRD patterns shows very strong agreement (Table S2†). The peaks give an approximate match to a cubic unit cell of dimension $a = 8.160 \text{ \AA}$. This may be compared with values $a = 8.238 \text{ \AA}$ for the cubic spinel LiMn_2O_4 ³² and $a = 8.143 \text{ \AA}$ for the spinel $\text{Li}_2\text{CoMn}_3\text{O}_8$.³³ Refinement of the structure of our preparation by first distorting the cubic cell to tetragonal and then tilting the tetragonal c -axis slightly results in a monoclinic unit cell with parameters $a = b = 5.774 \text{ \AA}$, $c = 8.148 \text{ \AA}$ and $\beta = 90.6^\circ$. This cell gives an excellent fit to the observed pattern. The present material is of monoclinic symmetry with $a = b = 5.774 \text{ \AA}$, $c = 8.148 \text{ \AA}$ and $\beta = 90.6^\circ$, in excellent agreement to both observed and simulated patterns.

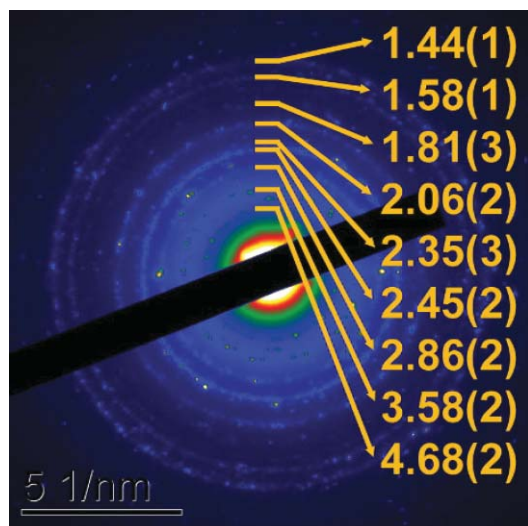


Fig. 5 Selected area electron diffraction pattern of a typical material. Major diffraction rings (in \AA) are highlighted.

Conclusions

We have demonstrated the first synthesis of a version of $\text{Li}_x(\text{Mn}_{1/3}\text{Ni}_{1/3}\text{Co}_{1/3})\text{O}_2$ in a periodic mesoporous form. This complex metal oxide required repeated application of a 'two solvents' pore infiltration technique, involving a mesoporous silica template that was filled by addition of an aqueous precursor solution to an anhydrous organic suspension of the silica. This pore filling mechanism proved substantially superior to more commonly used procedures. The material exhibits a surface area of *ca.* $180 \text{ m}^2\text{g}^{-1}$ with a pore size distribution centred at 5.5 nm and can be prepared in the temperature range of 500–700 °C. Selected

area electron diffraction revealed the complex phase to be very similar to a previously reported lithium manganate spinel.

Acknowledgements

This research was undertaken on the powder diffraction beamline at the Australian Synchrotron, Victoria, Australia. MRH thanks the CSIRO Science Leader Scheme and Hierarchical Materials Emerging Science Initiative for funding. Funding from the Victorian State Government for the JEOL 2100F microscope is acknowledged.

Notes and references

- 1 M. Armand and J. M. Tarascon, *Nature*, 2008, **451**(7179), 652.
- 2 F. Cheng, Z. Tao, J. Liang and J. Chen, *Chem. Mater.*, 2008, **20**(3), 667.
- 3 W. B. Yue and W. Z. Zhou, *Prog. Nat. Sci.*, 2008, **18**(11), 1329.
- 4 Z. P. Jiang, D. L. Jiang, J. X. Zhang and Q. L. Lin, *Prog. Chem.*, 2008, **20**(10), 1465.
- 5 J. N. Kondo and K. Domen, *Chem. Mater.*, 2008, **20**(3), 835.
- 6 T. Valdes-Solis and A. B. Fuertes, *Mater. Res. Bull.*, 2006, **41**(12), 2187.
- 7 B. Smarsly and M. Antonietti, *Eur. J. Inorg. Chem.*, 2006, (6), 1111.
- 8 D. Grosso, C. Boissiere, B. Smarsly, T. Brezesinski, N. Pinna, P. A. Albouy, H. Amenitsch, M. Antonietti and C. Sanchez, *Nat. Mater.*, 2004, **3**(11), 787.
- 9 H. Liu, Y. P. Wu, E. Rahm, R. Holze and H. Q. Wu, *J. Solid State Electrochem.*, 2004, **8**(7), 450.
- 10 F. Schuth and F. Marlow, *Nature*, 2007, **449**(7162), 550.
- 11 M. R. Hill, S. J. Pas, S. T. Mudie, D. F. Kennedy and A. J. Hill, *J. Mater. Chem.*, 2009, **19**, 2215.
- 12 K. M. Shaju and P. G. Bruce, *Adv. Mater.*, 2006, **18**(17), 2330.
- 13 J. Y. Luo, J. J. Zhang and Y. Y. Xia, *Chem. Mater.*, 2006, **18**(23), 5618.
- 14 C. S. Johnson, N. C. Li, C. Lefief and M. M. Thackeray, *Electrochem. Commun.*, 2007, **9**(4), 787.
- 15 S. H. Kang, P. Kempgens, S. Greenbaum, A. J. Kropf, K. Amine and M. M. Thackeray, *J. Mater. Chem.*, 2007, **17**(20), 2069.
- 16 J. Y. Luo, Y. G. Wang, H. M. Xiong and Y. Y. Xia, *Chem. Mater.*, 2007, **19**(19), 4791.
- 17 F. Jiao, J. L. Bao, A. H. Hill and P. G. Bruce, *Angew. Chem., Int. Ed.*, 2008, **47**(50), 9711.
- 18 F. Jiao, K. M. Shaju and P. G. Bruce, *Angew. Chem., Int. Ed.*, 2005, **44**(40), 6550.
- 19 X. Li, F. Cheng, B. Guo and J. Chen, *J. Phys. Chem. B*, 2005, **109**(29), 14017.
- 20 A. Rumpelcker, F. Kleitz, E. L. Salabas and F. Schuth, *Chem. Mater.*, 2007, **19**(3), 485.
- 21 M. Imperor-Clerc, D. Bazin, M. D. Appay, P. Beaunier and A. Davidson, *Chem. Mater.*, 2004, **16**(9), 1813.
- 22 D. Tonti, M. J. Torralvo, E. Enciso, I. Sobrados and J. Sanz, *Chem. Mater.*, 2008, **20**(14), 4783.
- 23 Y. S. He, Z. F. Ma, X. Z. Liao and Y. Jiang, *J. Power Sources*, 2007, **163**(2), 1053.
- 24 J. M. Tarascon and M. Armand, *Nature*, 2001, **414**(6861), 359.
- 25 K. S. Kang, Y. S. Meng, J. Breger, C. P. Grey and G. Ceder, *Science*, 2006, **311**(5763), 977.
- 26 J. Roggenbuck, T. Waitz and M. Tiemann, *Microporous Mesoporous Mater.*, 2008, **113**(1–3), 575.
- 27 5.00 g of mesoporous KIT-6 silica was dried overnight at 105 °C, and subsequently suspended in 300 mL dry hexane in a dry polypropylene flask under N_2 atmosphere. After the suspension had been stirred for 1 h, a 5M aqueous solution of manganese, nickel and cobalt nitrates in equimolar quantities was added dropwise over 2 h. The volume of aqueous solution added was equal to the total pore volume of the silica as derived from an N_2 adsorption isotherm. The pink powder was isolated and heated to 300 °C at a heating rate of 1°C min^{-1} , being maintained at this temperature for 120 min. This infiltration and decomposition cycle was repeated and followed by heating at 1°C min^{-1} to the final calcination temperature of 500–700 °C for 6 h. The silica template was removed from the black powder by mixing with 20 mL 2M NaOH solution ($4 \times 12 \text{ h}$) at room temperature, the solvent being removed as the supernatant liquid following centrifugation at each

- stage. The remaining powder was washed with water and ethanol to remove free sodium. Lithiation was carried out using 2 cycles of LiNO_3 melt in excess at 370°C for 12 h. Unreacted LiNO_3 was removed by repeated washing with water and ethanol.
- 28 B. D. Cullity, *Elements of X-Ray Diffraction*. 2nd edn, Addison-Wesley, Reading, 1978.
- 29 K. M. Shaju, G. V. S. Rao and B. V. R. Chowdari, *J. Electrochem. Soc.*, 2003, **150**(1), A1.
- 30 C. Lyness, B. Delobel, A. R. Armstrong and P. G. Bruce, *Chem. Commun.*, 2007, (46), 4890.
- 31 P. Schmidt-Winkel, W. W. Lukens, P. D. Yang, D. I. Margolese, J. S. Lettow, J. Y. Ying and G. D. Stucky, *Chem. Mater.*, 2000, **12**(3), 686.
- 32 A. Rougier, I. Saadoune, P. Gravereau, P. Willmann and C. Delmas, *Solid State Ionics*, 1996, **90**(1–4), 83.
- 33 H. Kawai and A. West, *J. Mater. Chem.*, 1998, **8**, 837.